Climate Dynamics (2000) 16:501–515

J. M. Gregory

Vertical heat transports in the ocean and their effect on time-dependent climate change

Received: 8 July 1999 / Accepted: 17 November 1999

Abstract In response to increasing atmospheric concentrations of greenhouse gases, the rate of time-dependent climate change is determined jointly by the strength of climate feedbacks and the efficiency of processes which remove heat from the surface into the deep ocean. This work examines the vertical heat transport processes in the ocean of the HADCM2 atmosphere–ocean general circulation model (AOGCM) in experiments with CO_2 held constant (control) and increasing at 1% per year (anomaly). The control experiment shows that global average heat exchanges between the upper and lower ocean are dominated by the Southern Ocean, where heat is pumped downwards by the wind-driven circulation and diffuses upwards along sloping isopycnals. This is the reverse of the low-latitude balance used in upwelling–diffusion ocean models, the global average upward diffusive transport being against the temperature gradient. In the anomaly experiment, weakened convection at high latitudes leads to reduced diffusive and convective heat loss from the deep ocean, and hence to net heat uptake, since the advective heat input is less affected. Reduction of deep water production at high latitudes results in reduced upwelling of cold water at low latitudes, giving a further contribution to net heat uptake. On the global average, high-latitude processes thus have a controlling influence. The important role of diffusion highlights the need to ensure that the schemes employed in AOGCMs give an accurate representation of the relevant sub-grid-scale processes.

1 Introduction

On physical grounds, it is expected that when the atmospheric CO_2 concentration is increased, the climate system warms up, because of the enhanced greenhouse effect. The nature of the response is investigated using computer models of the climate system. The global average temperature change in the steady state for a doubled CO_2 concentration is referred to as the "climate sensitivity", and has customarily been used as a parameter to compare the equilibrium response of different climate models (e.g. Mitchell et al. 1990). In recent years, however, the focus of climate prediction has moved to the time-development of climate change, rather than the eventual steady state (Bretherton et al. 1990; Gates et al. 1992). This is because our immediate practical interest lies in what the climate will be in the next few decades, during which time it will certainly not have reached a steady state. Moreover, we have little idea at what level CO_2 might stabilise. For time-dependent climate change simulation, one has to include the ocean, because of its enormous capacity to take up heat and retard climate change. The correct simulation of oceanic vertical heat transport processes is of comparable importance to the climate sensitivity in making a realistic prediction of time-dependent climate change.

In view of this, atmosphere–ocean general circulation models (AOGCMs) have now been developed and used by many authors for time-dependent climate prediction (e.g. Cubasch et al. 1992; Mitchell et al. 1995; Colman et al. 1995; Russell et al. 1995; Meehl and Washington 1996; Gordon and O'Farrell 1997; Haywood et al. 1997; Boer et al. 2000; Wood et al. 1999). Gregory and Mitchell (1997) compared the climate change simulated by the HADCM2 AOGCM (Johns et al. 1997) when run with and without flux adjustment in response to CO_2 increasing at 1% per year, and found that the temperature response of the unfluxadjusted model was smaller on the global average, although its geographical distribution was similar. Further analysis showed that about half this difference was due to the unfluxadjusted model's more effective vertical heat transports, which also led to deeper penetration of the warming. The need to understand these differences motivated a more detailed

J. M. Gregory
Hadley Centre for Climate Prediction and Research,
Meteorological Office, London Road, Bracknell,
Berks. RG12 2SY, United Kingdom
E-mail: jmgregory@meto.gov.uk

analysis of the relevant processes in each of the two models.

This work examines the vertical heat transports in the fluxadjusted HADCM2 ocean, with the objects of describing and accounting for the balance of terms in the control climate and the uptake of heat in time-dependent climate change. The control experiment (referred to as "FC" by Gregory and Mitchell 1997) is described by Johns et al. (1997). It is extremely stable, with a global average surface temperature drift of 0.16 K over a thousand years. Subsurface drifts are larger, but nonetheless small compared with the signal of climate change. The climate change experiment comprises an ensemble of four 80-year integrations each with CO_2 increasing at 1% per year compounded (referred to as "anomaly" in this work and "FA" by Gregory and Mitchell 1997). Having slightly different initial conditions, the four integrations rapidly diverge in detail, and thus provide four independent realisations of the climate. More details on the initialisation of the runs and the variability within the ensemble are given by Keen and Murphy (1997). The 1% scenario is adopted for the sake of simplicity; it is an approximation to expected future rates of CO_2 increase, but exhibits the cold-start effect (see Keen and Murphy 1997). The analysis concentrates on the last 20-year period, which is centred on the time when CO_2 reaches twice its initial concentration. The anomaly climate is taken as the ensemble mean of these 20 years, and the control climate as the average of the corresponding portions of the control run. The climate change is the difference between anomaly and control. The global average surface air temperature change is 1.8 K. The climate sensitivity is estimated as 2.6 K from the experiments discussed here (Gregory and Mitchell 1997). Senior and Mitchell (Submitted 2000) and Raper et al. Submitted (2000) discuss the time-dependence of climate sensitivity in HADCM2.

2 Identification of the upper ocean

The surface air temperature is closely linked in its time development to the temperature of the upper ocean. Understanding the heat balance of the upper ocean is therefore central to this work. If the ocean were a well-mixed layer of fixed depth (as in climate models with a "slab" ocean), an input of heat would produce a temperature change determined by the heat capacity of the slab. A larger heat capacity would give a smaller temperature change. From the temperature change ΔT (difference between anomaly and control states) we can evaluate the total heat taken up by the ocean as

$$\int_{-H}^{0} \oint c\Delta T(x,y,z)\mathrm{d}^2A\,\mathrm{d}z \qquad (1)$$

where c is the volumetric heat capacity, H the depth of the ocean at geographical location (x,y) and the surface integral is over the total ocean area A at level z (positive upwards, $z = 0$ at the surface). The heat uptake amounts to 7.5×10^{23} J. This quantity of heat would produce a temperature change of 1.0 K, equal to the HADCM2 global average SST change, when applied to a slab ocean with a depth of 480 m, which can therefore be regarded as indicating the effective heat capacity of the ocean (see Keen and Murphy 1997, who calculate this quantity in a time-dependent way). However, of course, the HADCM2 ocean is much deeper than 480 m, and the temperature change is not uniform through the column, the largest temperature rise being seen at the surface (Figs. 1, 2). The effective heat capacity is only a description, not an explanation; it measures the effectiveness of the processes which transport the heat downward through the water column. The aim of this work is to account for temperature change in terms of these processes.

Since we are concerned with the time-development of temperature change, we identify the upper ocean as a layer which shows temperature variations that are in-

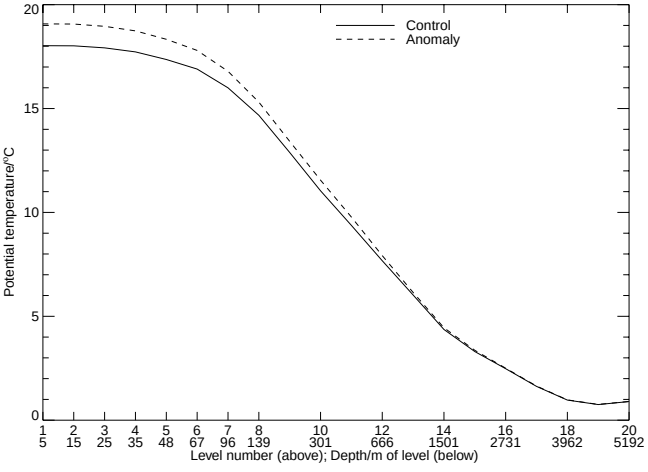

Fig. 1 Global average potential temperature as a function of depth

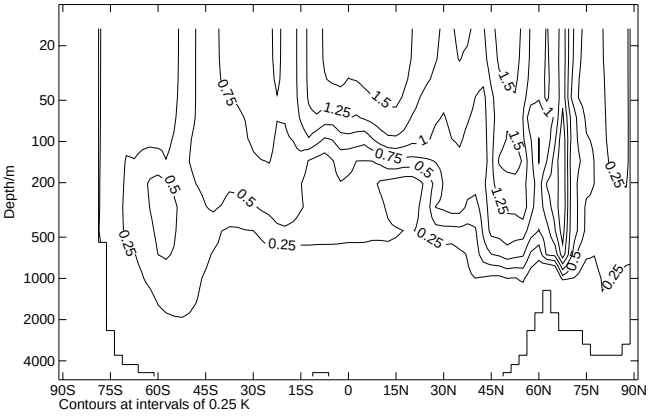

Fig. 2 Zonal-mean change in potential temperature as a function of depth and latitude between the control and anomaly climates

ternally coherent and correspond to surface temperature changes. We examine the temporal correlation of the heating rates for each ocean layer with the surface (top-layer) heating rate, evaluating the correlation coefficients from decadal means in the anomaly experiment, since we are concerned with temperature changes on the time scale of decades rather than shorter periods. There is strong correlation in the top 100 m (down to layer 7), and a sharp demarcation of an uncorrelated lower ocean (Fig. 3). (Note that the quantities correlated are rates of change of temperature, not temperatures. The temperatures themselves at *all* levels are strongly correlated, since the temperature at all depths is rising throughout the run, albeit with variability superimposed.)

Observations of ocean temperature profiles generally show an isothermal upper layer, referred to as the "mixed layer" (conventionally differing by less than 0.1 °C from the surface temperature), within which there are strong heat exchanges. However, the depth of the mixed layer is variable, both in time and space. It is shallower at low latitudes and in summer, on account of weaker winds and stronger stratification caused by insolation. No well-defined isothermal layer is apparent in the global average temperature profile (Fig. 1). Furthermore, there is only limited geographical similarity (not shown) between the mixed-layer depth and the penetration of temperature change. The mixed layer is therefore not an appropriate definition of the upper ocean.

The heat content of the upper ocean is determined by the surface net heat flux into the ocean and the loss of heat to the lower ocean. The surface heat input increases roughly linearly in time during the anomaly experiment (Fig. 4). We examine the distribution with depth of the accumulated heat by dividing the heat storage below level z

$$\int_{-H}^{z} \oint c\Delta T(x,y,z')\mathrm{d}^2A\,\mathrm{d}z' \qquad (2)$$

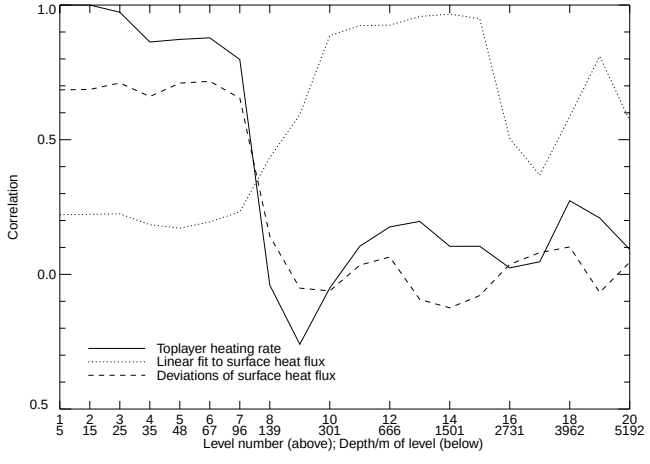

Fig. 3 Temporal correlation of the heating rate as a function of depth with the top-layer heating rate and the surface heat flux

by the total heat uptake (Eq. 1). We find that only 10% is retained in the top 50 m (5 layers) and 25% in the upper 160 m (8 layers) (Fig. 5). Most of the surface heat input passes into the lower ocean. Therefore, as the surface heat flux grows, the upper ocean must be losing an increasing and nearly equal heat flux to the lower ocean. The heating rate of the upper ocean, which is the difference between these two fluxes, is small on average compared with either of them.

Like the surface heat input, the upper ocean temperature increases roughly linearly with time (Fig. 6). Hence, as observed by Gregory and Mitchell (1997), the heat flux into the deep ocean is proportional to the temperature change. The physical interpretation is that, having little heat capacity, the upper ocean increases its temperature so as to increase the rate of heat loss to the lower ocean, and balance the surface heat flux.

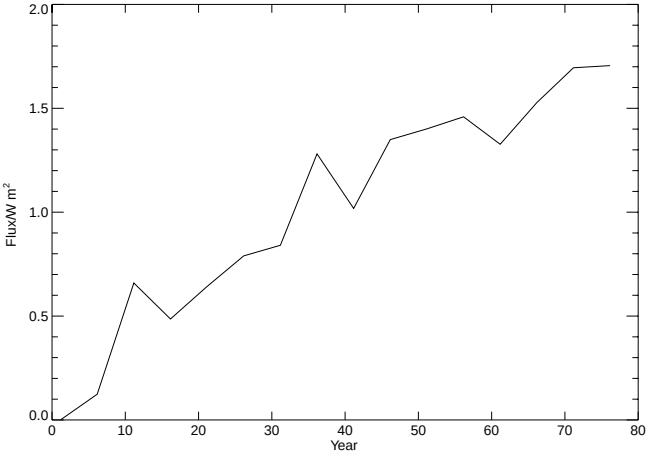

Fig. 4 Global average net heat flux into the ocean as a function of time during the anomaly experiment (power per unit area of the world ocean)

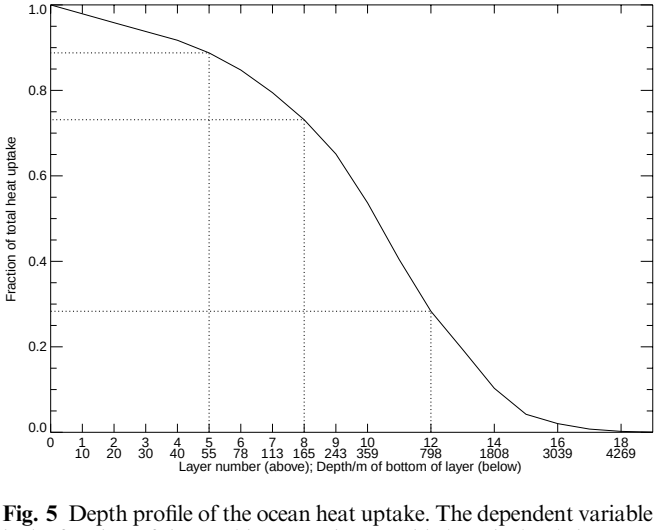

Fig. 5 Depth profile of the ocean heat uptake. The dependent variable is the fraction of the total heat uptake stored below the level shown as the independent variable

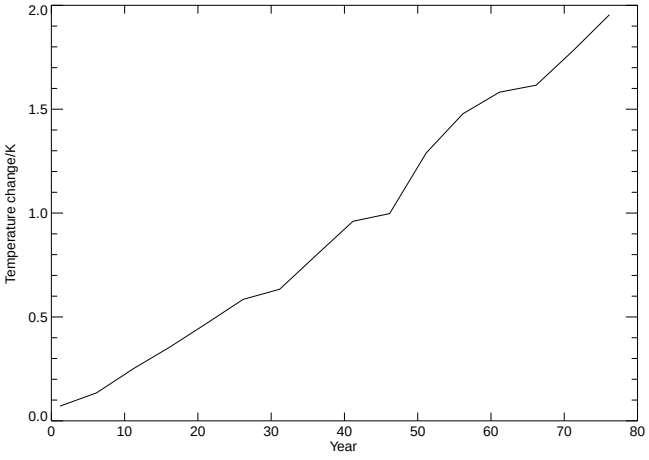

Fig. 6 Global average surface air temperature change as a function of time during the anomaly experiment

The temperature of the lower ocean rises by much less, so the increase in the temperature difference between them is mostly due to the warming in the upper ocean. On the other hand, despite its small temperature change, the majority of the extra heat resides in the lower ocean, on account of its large heat capacity.

These qualitative explanations of the partitioning of the heat can be related to the depth dependence of the heating rate correlations by reference to a quantitative model, in which we divide the ocean into two layers, the vertical heat flux between them being proportional to their temperature difference. The formulation of the model and its solutions are given in Appendix A. Choosing parameters appropriate to the time-development of the anomaly experiment confirms that fluctuations of the surface heat flux on a decadal time scale should affect the temperature of an upper layer of thickness 100–200 m, while the heat flux into the lower layer increases fairly steadily. In the remainder of this work we focus on the vertical heat flux at 160 m (the base of layer 8) to account for the time-development of the SST. This definition of the upper ocean is somewhat arbitrary, but the qualitative conclusions of the analysis would be unaltered if we made a slightly different choice.

Because the surface heat flux increases linearly with time t, the additional heat content of the entire ocean rises like t^2. This quadratic increase is shown by Bryan (1996) (the slope of his logarithmic plot of $\Delta\theta$ against time in his Fig. 2b is close to 2). He indicates that the additional heat content would increase like $t^{3/2}$ for a uniformly conducting ocean with surface temperature increasing linearly with time, as ours and his do. However, our picture of the ocean is not of a uniform conductor, but of two distinct layers, and the SST is a property of a part of the ocean with effectively negligible heat capacity, a "skin" temperature, on decadal time scales, and hence relates, as we have seen, to the heat flux into the ocean, and not to the heat contents of the ocean.

3 Global average vertical heat transfer processes

Within the HADCM2 ocean, heat is transported by three kinds of process: advection, diffusion and vertical mixing. All three of these processes are conservative, in that they do not change the total heat content of the ocean; vertical mixing redistributes heat only within each column, but advection and diffusion move it horizontally as well. We diagnose the rate of heating in $\mathrm{K\,s^{-1}}$ caused by each of these processes on each time step during an integration of HADCM2. These heating rates can be converted to heat convergences in $\mathrm{W\,m^{-3}}$ by multiplying by the volumetric heat capacity ($4.1 \times 10^6\,\mathrm{J\,m^{-3}\,K^{-1}}$), and to $\mathrm{W\,m^{-2}}$ by integrating over a range of depths.

In the control, the ocean is practically in a steady state, implying zero global average vertical net flux at all levels. (A steady state requires zero vertical divergence of the heat flux. Since the heat flux is necessarily zero at the bottom of the ocean in the model, which does not include any heat exchange through the ocean floor, it must vanish at all depths.) The steady state is maintained by a balance of opposing influences (Fig. 7). The dominant terms each have a magnitude of a few $\mathrm{W\,m^{-2}}$ down to depths of 2000 m. These represent very large fluxes, $1\,\mathrm{W\,m^{-2}}$ over the entire ocean surface amounting to 0.36 PW in total, about 30% of the meridional transport at 24°N in the Atlantic, for instance (Hall and Bryden 1982).

At all depths in the global average, advection transports heat downwards. Advection is the movement of heat by the velocity field i.e. the motions which are resolved and explicitly modelled. Downward advective transport means that sinking water is warmer than rising water, on average.

Vertical mixing and diffusion move heat upward on the global average. This is a surprising observation for diffusion, since the ocean is cooler at greater depth, so an

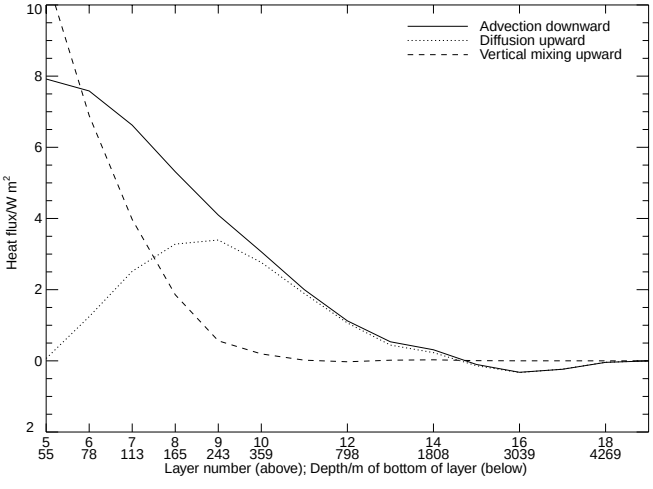

Fig. 7 Global average vertical heat fluxes in the control climate (power per unit area of the world ocean)

upward heat transfer is counter-gradient. HADCM2 has two schemes which diffuse heat vertically (Johns et al. 1997):

1. Diffusion within neutral surfaces, with a diffusivity that varies with vertical coordinate z as $400 + 1600\exp(z/500)\,\mathrm{m^2\,s^{-1}}$. The distinction between neutral and isopycnal surfaces (McDougall 1987) is not qualitatively important to the conclusions of this work, so we will refer to such diffusion as "isopycnal".
2. Diffusion within the vertical column, with a diffusivity increasing from about $10^{-5}\,\mathrm{m^2\,s^{-1}}$ near the surface to $10^{-4}\,\mathrm{m^2\,s^{-1}}$ around 4000 m. As isopycnal surfaces are roughly horizontal, we will refer to this process as "diapycnal" for clarity and convenience.

Diapycnal diffusion could not give the observed effect, which comes about through diffusion along isopycnals that slope because of salinity gradients, as will be shown later (Sect. 5).

The result shown here of downward advection balancing upward diffusion is the reverse of the picture presented by one-dimensional upwelling–diffusion ocean models, such as those of Hoffert et al. (1980), Schlesinger and Jiang (1990) and Wigley and Raper (1992), in which heat diffusing downward from the surface is balanced by the upwelling of cold water. This idea properly applies to low latitudes, as we will see (Sect. 7), but it does not correctly represent the global ocean, which is dominated by vertical exchanges at high latitudes.

Above 400 m, vertical mixing is important, and it is the largest term in the mixed layer. This is not unexpected, because the bulk mixing of water by convection or the wind is more effective than the small-scale turbulence represented by vertical diffusion. On the global average, the heat flux is upward because vertical mixing is dominated by convection driven by surface cooling, or by brine rejection during sea-ice formation in a cold surface layer with underlying warmer water. In principle, convection driven by the salinification of a warm surface layer could transfer heat downward, but this is unlikely because when the water is warm the effect of salinity on density is relatively weak. (We discuss this effect in more detail in Sect. 5.) In HADCM2, vertical mixing is represented by two schemes. The mixed-layer parametrisation of Kraus and Turner (1967) produces an isothermal layer from the surface to a depth determined by the energy input by the wind and released by convection. Convection initiated from beneath the surface is modelled by the convection scheme of Cox (1984).

The differences between anomaly and control in the global average fluxes are an order of magnitude smaller than the fluxes in the control (Fig. 8). In this case also, the upwelling–diffusion picture of the ocean does not serve us well, since the additional downward net heat flux is conveyed from the surface by advection as well as diffusion. There is a reduction of heat loss by diffusion in the global average, and this change is the dominant effect below about 500 m. The upward transfer of heat by vertical mixing is also reduced, which would be consistent with greater stability caused by surface warming. Unlike in the control, the terms clearly do not sum to zero, and the net downward heat flux, decreasing with depth, warms the interior of the ocean.

4 Latitudinal variation of vertical heat transfer processes

We now examine the latitudinal variation of the vertical heat transfer processes across a surface at 160 m, which we have defined as the base of the upper ocean. From the control model output we diagnose the heat convergence in the water column below this depth as a function of latitude for each of the processes separately (Fig 9). For the vertical mixing processes, the heat convergence equals the vertical heat flux across 160 m, since they do not transport heat horizontally, but for advection and diffusion, the heat convergence includes a meridional

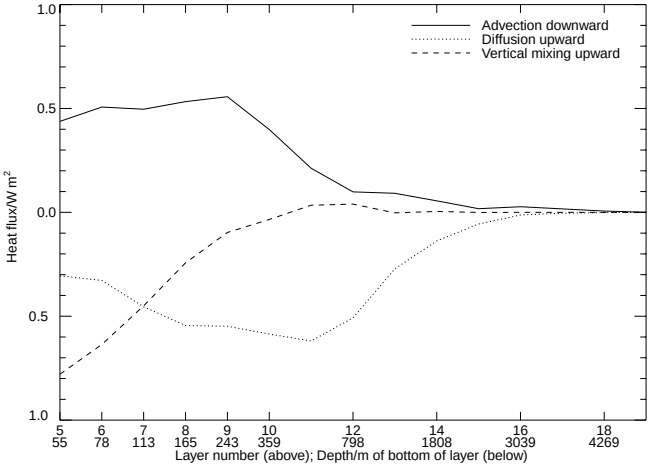

Fig. 8 Changes in global average vertical heat fluxes between the control and anomaly climates (power per unit area of the world ocean)

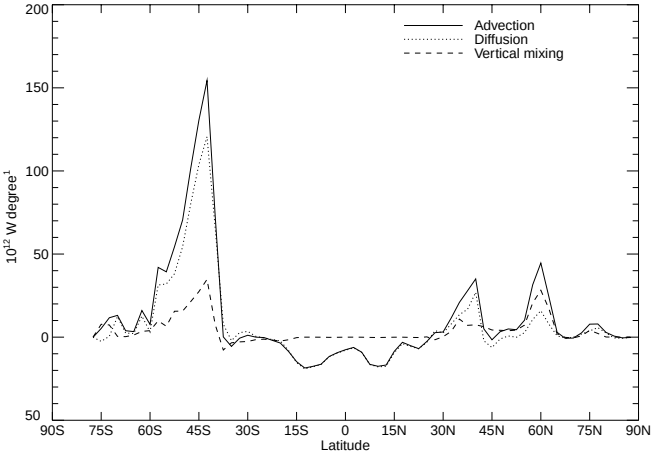

Fig. 9 Heat convergence below 160 m as a function of latitude in the control climate. Advection is shown as positive for heating, diffusion and vertical mixing as positive for cooling

term and hence is not equal to the vertical heat flux. (Since we integrate over all longitudes, there is no zonal term in the heat convergence as a function of latitude.) The meridional diffusive heat flux is relatively small. The decomposition of the advective heat flux into components is problematic. The difficulty and the scheme adopted in subsequent sections are described in Appendix B.

To investigate advective heat transports further, we need to be able to recalculate them outside the model, so that we can vary the inputs at will and see how the result is affected. Advection involves the product of velocity and temperature, and in general the product of time-means will not equal the time-mean of a product. However, the recalculation of advective heating below 160 m from decadal means is closely equal to the diagnosis from the model. That implies that most of the heat convergence below 160 m is due to the mean flow; time-variation does not matter much. (Fanning and Weaver 1997 found the same for the Atlantic meridional transport.)

The world is divided into three major latitude bands according to the different ways in which a heat balance is achieved. At low latitudes (between 30°N and 30°S), the ocean below 160 m is cooled by advection and heated by diffusion. In the Southern Ocean (south of 30°S), advection is a heating effect, balanced mainly by diffusive cooling and partly by vertical mixing. In the northern oceans (north of 30°N), there is a similar picture, but vertical mixing is relatively more important. Off-line calculations indicate that vertical diffusion at low latitudes is diapycnal, and at high latitudes isopycnal.

In Table 1 we show the contribution of each heat transfer process to heat convergence below 160 m in each of the three latitudinal bands, separated by ocean basin, in the control and for the difference between anomaly and control. Since the control is nearly in a steady state (the global average surface heat flux is $0.18\,\mathrm{W\,m^{-2}}$ into the ocean), the total heat convergence in each latitude–basin box is close to zero. This is obviously not true for the anomaly and hence not for their difference; Table 1 shows the processes which take up heat in the ocean below 160 m during climate change. In the following sections we discuss the balance in the control and the perturbation to that balance in each of the latitude bands in turn.

5 Southern Ocean

The largest vertical exchanges of heat occur in the Southern Ocean (Fig. 9). Here, isopycnal diffusion cools the lower ocean because of two circumstances. Firstly, the water is cold. Thermal expansivity declines strongly with temperature T, but the dependence of density on salinity S varies relatively little over the ranges encountered in the ocean (e.g. see Appendix 3 of Gill 1982). Hence at low temperatures, salinity becomes a relatively more important influence on density. For the distributions of T and S in the Southern Ocean, density is mostly determined by salinity; heat is nearly a passive tracer. Secondly, the vertical temperature gradient is weak in the Southern Ocean. As a consequence of these together,

Table 1 Heat convergence below 160 m

Latitude	Process	Global		Atlantic		Pacific		Indian	
		C	A–C	C	A–C	C	A–C	C	A–C
90°S–90°N	Total	0.15	1.31	0.00	0.44	0.10	0.50	0.05	0.37
	Advection	5.27	0.53	3.42	−0.03	0.22	0.25	1.63	0.31
	Diffusion	−3.27	0.54	−1.96	0.23	−0.10	0.20	−1.20	0.10
	Vertical mixing	−1.84	0.24	−1.46	0.24	−0.02	0.05	−0.37	−0.05
90°S–30°S	Total	0.04	0.55	−0.02	0.14	0.03	0.20	0.02	0.21
	Advection	4.97	0.11	2.51	−0.16	0.57	0.14	1.89	0.13
	Diffusion	−3.90	0.44	−1.75	0.22	−0.67	0.10	−1.48	0.12
	(Vertical diffusion)	−4.01	0.41	−1.82	0.22	−0.69	0.09	−1.50	0.10
	Vertical mixing	−1.03	0.00	−0.77	0.08	0.13	−0.04	−0.39	−0.04
30°S–30°N	Total	0.10	0.59	0.03	0.20	0.04	0.24	0.03	0.16
	Advection	−1.35	0.50	−0.21	0.18	−0.88	0.14	−0.26	0.18
	Diffusion	1.35	0.08	0.22	0.01	0.86	0.09	0.28	−0.02
	(Vertical diffusion)	1.52	0.10	0.29	0.00	0.91	0.10	0.32	0.00
	Vertical mixing	0.09	0.01	0.02	0.01	0.06	0.00	0.01	0.00
30°N–90°N	Total	0.01	0.16	−0.01	0.11	0.02	0.06		
	Advection	1.65	−0.09	1.12	−0.05	0.52	−0.04		
	Diffusion	−0.72	0.02	−0.43	0.00	−0.29	0.01		
	(Vertical diffusion)	−0.79	0.03	−0.45	0.02	−0.34	0.01		
	Vertical mixing	−0.91	0.24	−0.70	0.15	−0.21	0.09		

Each entry shows the vertical integral below 160 m of the heat convergence, expressed in $\mathrm{W\,m^{-2}}$ averaged over the global ocean area. The rows marked 'Total' are the sum of the values for advection, diffusion and vertical mixing (Diffusion includes Vertical diffusion). The columns marked 'C' apply to the control climate, A–C to the difference between the anomaly and the control. 'Global' indicates the sum over all ocean basins. The Arctic Ocean is included in the Atlantic Ocean. Note that the Indian Ocean does not extend as far as 30°N. Marginal and inland seas are excluded

relatively warmer deep water has the same density as colder fresher water nearer the surface at higher latitudes, so the isopycnals cut across the isothermals (Fig. 10) and produce an isopycnal temperature gradient which is warmer downwards (Osborn 1998; Guilyardi et al. 1999).

We can show how this arises with a rough calculation. At 160 m within 40–60°S, the latitude band of large upward diffusive flux (Fig. 9), the average temperature gradients are $2 \times 10^{-3}\,\mathrm{K\,m^{-1}}$ vertically (warmer upwards) and $5 \times 10^{-6}\,\mathrm{K\,m^{-1}}$ meridionally (colder southwards). The isopycnals slope upwards to the south with an average gradient of 10^{-3}. The southward isopycnal temperature gradient is therefore negative, being the sum of $-5 \times 10^{-6}\,\mathrm{K\,m^{-1}}$, almost the entire meridional gradient, and $+2 \times 10^{-6}\,\mathrm{K\,m^{-1}}$, one-thousandth of the vertical gradient (Fig. 11). Hence heat diffuses southward and upward, as anticipated. At this depth, the isopycnal diffusivity is $1500\,\mathrm{m^2\,s^{-1}}$, so the upward component of the isopycnal diffusive flux (the product of the slope, isopycnal temperature gradient, diffusivity and volumetric heat capacity) will be $10^{-3} \times 3 \times 10^{-6} \times 1500 \times 4 \times 10^6 = 18\,\mathrm{W\,m^{-2}}$. The diapycnal diffusivity is $2 \times 10^{-5}\,\mathrm{m^2\,s^{-1}}$, so the downward diapycnal flux will be $2 \times 10^{-3} \times 2 \times 10^{-5} \times 4 \times 10^6 = 0.2\,\mathrm{W\,m^{-2}}$, a hundred times smaller. Diapycnal diffusion is hence negligible in these latitudes.

The area-average diagnosed upward diffusive heat flux at 160 m in the Southern Ocean is $3.90\,\mathrm{W\,m^{-2}}$ (Table 1, power per unit area of the world ocean, as for all vertical heat fluxes henceforth). This diffusive cooling is mostly balanced by advective warming, resulting from vertical heat exchange by the Deacon cell, which pumps water downwards around 30°S and upwards around 60°S, as pointed out by Manabe et al. (1991). The descending water is warmer, which is possible because the cell is driven not by density, but by the latitudinal variation of the windstress $\boldsymbol{\tau}$. We can demonstrate this by calculating the integral of the Ekman suction velocity $\mathbf{k} \cdot \nabla \times (\boldsymbol{\tau}/\rho f)$ ($\mathbf{k}$ being a vertical unit vector, ρ density and f the Coriolis parameter) over the area between the Antarctic coast and 45°S, where it changes its sign. This amounts to 45 Sv, nearly equal to the volume flux of 47 Sv circulating in the Deacon cell (Fig. 12). The advective heating of the water below 160 m in the Southern Ocean amounts to $5.0\,\mathrm{W\,m^{-2}}$, of which we can ascribe $4.7\,\mathrm{W,m^{-2}}$ to the vertical exchanges across this level, using the technique described in Appendix B. Meridional exchanges at 30°S account for the remainder, which is smaller because the meridional temperature gradient is weak below 160 m, whereas the contrast is strong between the temperatures of the sinking and rising branches of the vertical recirculation.

The advective heat divergence can be decomposed into zonal-mean and "eddy" contributions (denoted by [ ] and $'$ respectively), thus:

$$\begin{aligned}\nabla \cdot (\mathbf{v}T) &= \nabla \cdot (([\mathbf{v}] + \mathbf{v}')([T] + T')) \\ &= \nabla \cdot ([\mathbf{v}][T]) + [\mathbf{v}] \cdot \nabla T' + \mathbf{v}' \cdot \nabla [T] \\ &\quad + \nabla \cdot (\mathbf{v}'T') \ . \end{aligned} \tag{3}$$

In this context, "eddies" means stationary deviations from the zonal pattern, since we are always using time-

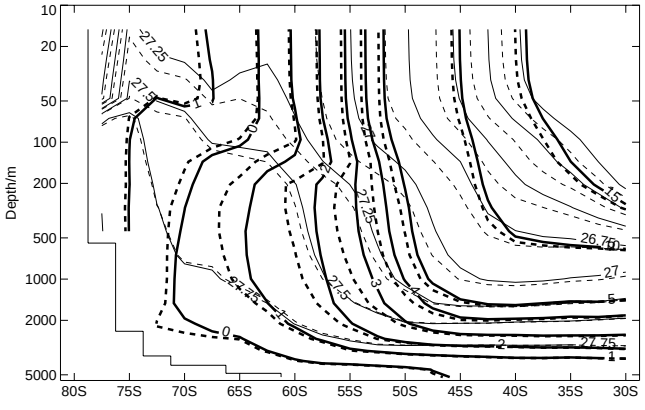

Fig. 10 Zonal-mean potential temperature and density as a function of depth and latitude in the control climate. Isothermals are shown as thick lines at intervals of 1°C upto 5°C, and then at intervals of 5°C. Isopycnals are shown as thin lines at intervals of 0.25 kg $\mathrm{m^{-3}}$. The control climate is shown as solid lines, the anomaly climate as dasheds

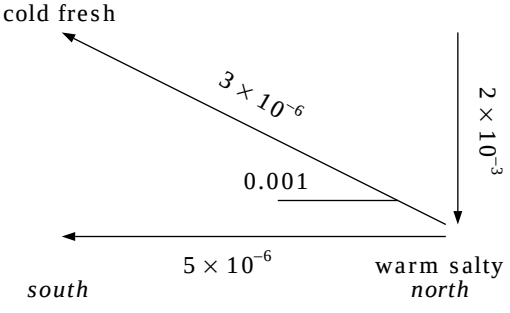

Fig. 11 Schematic showing the isopycnal temperature gradient in the Southern Ocean. Arrows point in the direction of heat flow, from warmer to colder

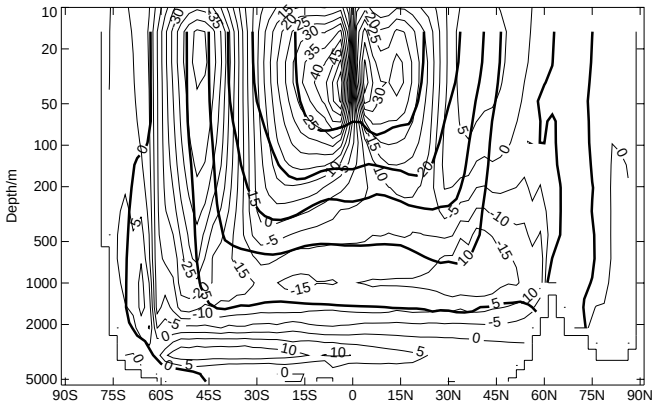

Fig. 12 Zonal-mean potential temperature and meridional overturning stream function as a function of depth and latitude in the control climate. Isothermals are shown as thick lines at intervals of 5°C. Stream lines are shown as thin lines at intervals of 5 Sv

mean fields. Upon calculating the zonal average heat convergence,

$$[\nabla \cdot (\mathbf{v}T)] = \nabla \cdot ([\mathbf{v}][T]) + \nabla \cdot ([\mathbf{v}'T']) \ , \qquad (4)$$

the cross-terms disappear. We can evaluate the first term on the right using the zonal-mean temperature and velocity fields. This gives a similar depth–latitude distribution of heating to the total (not shown), and a heat convergence of $3.8\,\mathrm{W\,m^{-2}}$, which is 25% less. A similar figure can be arrived at by a rough calculation. In HADCM2, the upward volume flux across the surface at 160 m south of 45°S is 38.6 Sv, and the downward flux between 30°S and 45°S is 37.4 Sv, the similarity of these indicating that there is little depth-integrated meridional flow across 30°S below 160 m. On this level, the average temperatures in the rising and sinking latitude bands are 3.1 °C and 13.1 °C. The heat pumped downwards is the product of 38 Sv with 10 °C (the temperature difference) and the volumetric heat capacity. When divided by the world ocean area, this gives a flux of $4.2\,\mathrm{W\,m^{-2}}$. These calculations demonstrate that in HADCM2 the zonal-mean overturning cell is responsible for most of the vertical heat transport; stationary eddies are relatively unimportant.

In some models of the ocean circulation (Döös and Webb 1994; Hirst et al. 1996b, also suggested by Karoly et al. 1997) it has been found that the Deacon cell is a circulation along isopycnal surfaces. Because these surfaces tend to be shallower on the eastern side of each ocean basin (see Osborn 1998), a circulation which flows north on the east and south on the west of each basin would look like an overturning cell when viewed in latitude–depth coordinates. Such a cell will not be apparent if the meridional stream function is evaluated in latitude–density coordinates instead, by summing over longitudes on isopycnal surfaces rather than surfaces of constant depth. In HADCM2, this procedure does still show the Deacon cell (Fig. 13), with a reduced intensity of 30–35 Sv, centred on about 50°S and $1026.9\,\mathrm{kg\,m^{-3}}$, a density surface which lies at around 200 m depth at most longitudes. Hence our Deacon cell can transport heat diapycnally.

This diapycnal advection must be balanced by some other diapycnal processes in a steady state. Since diffusion is isopycnal, the balance is with convection, which closes the budget in the control climate by transporting $1.0\,\mathrm{W\,m^{-2}}$ upwards across the 160 m surface.

Below 800 m, the diffusive cooling and advective warming are nearly balanced, convection being only a minor effect. Thus, in the deep ocean, the advective circulation must be nearly isopycnal. The advective heat convergence is diagnosed as $1.42\,\mathrm{W\,m^{-2}}$ and recalculated as 1.6 off-line, of which 0.9 is vertical and 0.7 horizontal, the latter resulting from intrusion of around 10 Sv of North Atlantic Deep Water below about 1200 m and from exchange with lower latitudes in the underlying bottom cell.

Changes in the Southern Ocean are responsible for 40% of the global heat uptake below 160 m in the anomaly experiment. The main effect is a reduction of $0.44\,\mathrm{W\,m^{-2}}$ in the upward diffusive heat flux, most pronounced around 140 m depth and between 50–60°S. This comes about because the isopycnal temperature gradient is reduced; in the anomaly climate the isopycnals are not much changed from the control, while the isothermals slope less steeply, on account of a subsurface warming (Fig. 2). In the zonal mean, the warming has a maximum 0.5 K in the zonal mean between 200–600 m depth and latitudes 55–65°S, and can be seen from the poleward "bulging" of the isothermals (Fig. 10). The isopycnals are similar in the two experiments because the salinity, the dominant influence on density, is little different.

If we choose a depth which is substantially below the mixed layer, such as 800 m, the reduction in the upward diffusive heat flux can be accurately recalculated from time-mean T and S fields and compares well with the model diagnostics in its geographical distribution. We confirm that the reduction is due to the temperature change by calculating the heat loss with altered temperatures and unchanged densities, and vice-versa. The latter gives little change, but the former is similar to the diagnosed change, except that it shows an overestimate of the change north of 50°S. This is probably because in this somewhat warmer region the

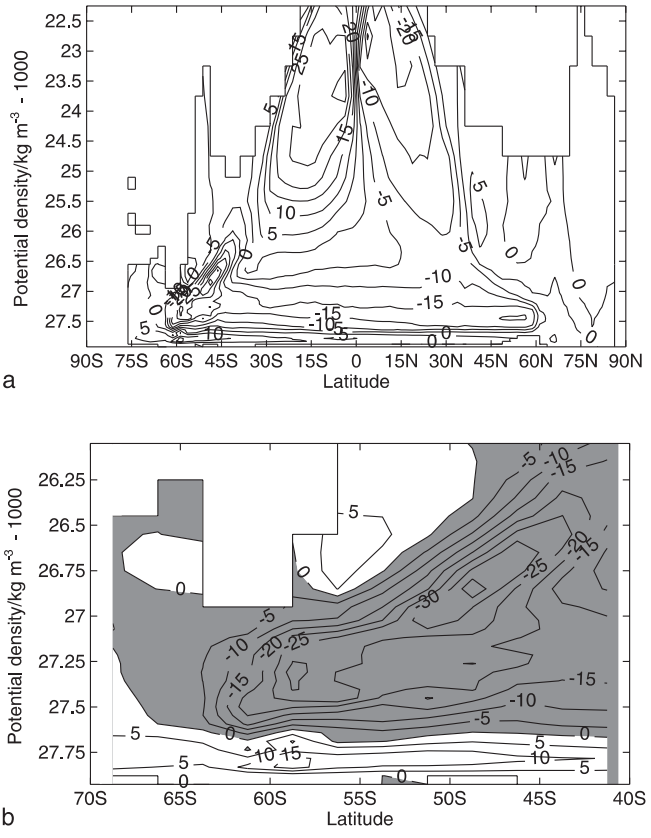

Fig. 13a, b Meridional overturning stream function as a function of potential density and latitude in the control climate: **a** world ocean (excluding marginal and inland seas); **b** Southern Ocean. Stream lines are shown at intervals of 5 Sv. Negative regions are shaded

raised temperatures do cause a reduction in density that also has a significant effect on the isopycnal temperature gradient.

In the Southern Ocean, the ocean warms the atmosphere; surface cooling drives convection, which compensates for the heat loss from the top layer by extracting heat from layers below. It is evident in layers 2–9 as a cooling by vertical mixing in these layers (Fig. 14), and produces a well-defined mixed layer, indicated by vertical isothermals (Fig. 10). Brine rejection during winter ice formation also helps drive the mixing.

As we have seen, there is an upward diffusive supply of heat from the deep ocean, leading to a temperature maximum around 200 m. Diffusion conveys this heat up to the mixed layer, thus producing cooling below layer 9 and warming above (Fig. 14). There is a transitional region between 100 and 300 m in which diffusion and vertical mixing both contribute to upward heat transport, balancing surface cooling against heating from beneath.

In the anomaly climate, Southern Ocean convection is weakened (as also found by, for instance, Manabe et al. 1991; Murphy and Mitchell 1995; Hirst et al. 1996a), so the rate of heat loss through the mixed layer declines, and heat accumulates underneath it, intensifying the temperature maximum and reducing the isopycnal temperature gradient, as discussed already. Convection is weakened because the surface buoyancy flux becomes less negative, 70% of the change being accounted for by a decrease of $0.50\,\mathrm{W\,m^{-2}}$ (expressed as a global average) in the surface heat loss, the remainder resulting mostly from increased precipitation, with a minor contribution at high latitudes from reduced sea-ice formation. Weaker convection caused by reduced heat loss would probably be associated with surface warming, whereas some of the areas with the greatest reductions in heat loss actually show surface cooling, likely to be a result of reduced heat transport to the surface by convection. Sensitivity tests such as those performed by Mikolajewicz and Voss (1998) for the north Atlantic would enable us to tell whether the thermal buoyancy flux change is a cause or a consequence of weakened convection. In any case, we may draw the conclusion that, through their effect on convection, surface flux changes are the cause of the smaller diffusive heat loss and the consequent increase to heat storage in the Southern Ocean below 160 m in the anomaly climate.

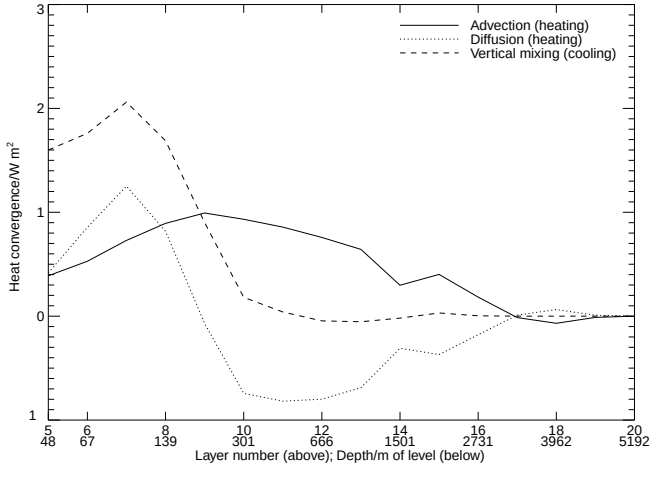

Fig. 14 Heat convergence as a function of depth in the Southern Ocean in the control climate

6 Northern Oceans

The oceans north of 30°N contribute least to heat uptake in climate change (Table 1), which is at first sight surprising because of the important role of the Atlantic thermohaline overturning circulation in global heat transport and its influence on the climate of Europe in particular. The Atlantic does indeed dominate the vertical heat exchanges in this latitude zone. Convection driven by surface heat loss warms the upper layers and cools the ocean beneath, maintaining a meridional density gradient at depth which drives the Atlantic overturning cell (e.g. Rahmstorf 1996). In HADCM2, the convection takes place mostly to the south of the Greenland–Iceland–Scotland ridges and in the Labrador Sea. The convection is intense within this small region, and the resultant upward heat flux has local values of several tens of $\mathrm{W\,m^{-2}}$ at 160 m, contributing more than a third of the global heat flux from vertical mixing ($0.70\,\mathrm{W\,m^{-2}}$, Table 1, power per unit area of the world ocean, as usual). By mixing denser with lighter water, convection produces a downward mass flux, but no volume flux; the vertical velocity in the downward branch of the circulation belongs to the large-scale motion driven by the density contrast.

In a steady state, the convective cooling beneath must be balanced by a supply of heat. This is provided by the large-scale circulation. The water which is drawn northwards and downwards in the north Atlantic is warmer than that which returns to the south as North Atlantic Deep Water, because of the heat which it gives up on its passage. Analysing the advective heat fluxes of the Atlantic below 160 m and between 30°N and 64°N (up to the latitude of Iceland) by the method of Appendix B, we find that the advective convergence of $1.0\,\mathrm{W\,m^{-2}}$ consists of 1.4 from exchange with the south, −0.2 with the north (across the ridges to the Nordic Seas) and −0.2 with the surface layers. The total convergence in this box is in good agreement with the diagnosed value of $0.9\,\mathrm{W\,m^{-2}}$ (smaller than the figure of 1.12 in Table 1 for the north Atlantic and Arctic because we are here considering a more restricted region).

In the north Atlantic, as in the Southern Ocean, there is also an upward isopycnal diffusive heat flux across 160 m, but it is less important than convection. Diffusion plays a lesser role than in the Southern Ocean, probably because the water is warmer in the Northern Hemisphere. For instance, at 160 m the zonal-mean temperature is about 1 °C at 60°S and about 7 °C at

60°N in the Atlantic sector. At these higher temperatures, temperature has a stronger effect on density, so a strong isopycnal temperature gradient cannot easily develop.

Convection also occurs in the north Pacific, but it is weaker ($0.21\,W\,m^{-2}$) and does not extend to such depth. This may be the main reason why there is no zonal-average meridional circulation in the Pacific in HADCM2, as in the real world, but the explanation of this difference between the Atlantic and the Pacific is a complicated subject (Weaver et al. 1999). The northward advective heat transport at 30°N in the Pacific (0.20 PW) is a good deal less than in the Atlantic (0.74 PW), and is associated with the wind-driven gyre rather than with density-driven overturning (see Bryden 1993).

The largest change to the northern oceans in the anomaly experiment is a reduction of convection. This is probably due both to a greater surface freshwater flux at high latitudes, where precipitation increases more than evaporation, and to weaker surface cooling, because of the warming of land relative to ocean and the retreat of sea-ice (see Mikolajewicz and Voss 1998). The upward heat flux from vertical mixing across 160 m decreases by 20% ($0.15\,W\,m^{-2}$) in the north Atlantic and 40% ($0.09\,W\,m^{-2}$) in the north Pacific, a reduction of $0.24\,W\,m^{-2}$ in total.

The meridional circulation is weaker in the anomaly experiment, as is found in most AOGCM experiments of this kind (e.g. Manabe and Stouffer 1994; Murphy and Mitchell 1995; Gordon and O'Farrell 1997; Boer et al. 2000). This is very likely to be a consequence of the reduction in convection, and it is the probable reason for the smaller advective heat transport. For the Atlantic within 30–64°N and below 160 m (the box considered already), we find that the heat convergence decreases by 10% ($0.1\,W\,m^{-2}$), similar to the reduction of 15% in the strength of the overturning circulation, from 20 Sv to 17 Sv. An off-line recalculation of the advective heating of this box confirms that the decrease is due to the change in $\mathbf{v}$ (slowing of the circulation) rather than the change in T (decrease of the temperature gradient) (see Murphy 1995, who made a similar observation for an earlier Hadley Centre model).

Thus, in the north Atlantic we see reduced convection. This has the direct effect of reducing heat loss by the ocean below 160 m. It also has an indirect effect of reducing heat uptake through the weakening of the thermohaline circulation, but this indirect effect is locally less important, so the net result is that heat storage in the north Atlantic ocean is increased. (However, the indirect effect extends to lower latitudes, as described in the next section.) Convection responds immediately to altered surface fluxes, and the circulation change is fairly rapid. The balance between convective heat loss and advective heat convergence in the deep ocean could be regained by an adjustment to the temperature gradients over the considerably longer time scale on which temperature anomalies are advected around by the gyre.

7 Low latitudes

Between 30°N and 30°S in the lower ocean there is a balance between cooling by advection and warming by diffusion. (Figure 15 is a diagram showing the various advective transports referred to in the following.) As a function of latitude, these terms are closely matched at 160 m, vertical mixing being more than ten times smaller than either (Fig. 9). Isopycnal diffusion is negligible at low latitudes, since the density variation is dominated by temperature, and isopycnals and isothermals are practically parallel and horizontal. Diffusion is diapycnal, being caused by the strong vertical temperature gradient maintained by advection, as described in the following paragraphs. In these latitudes, the off-line calculation of advective heat fluxes is very accurate, which enables us to analyse them in detail.

Analysis of zonal-mean advective fluxes by the method of Appendix B shows that meridional transports are important in the heat budget of the upper ocean, but with differences between basins. In the Atlantic basin at 30°S, there is northward flow in the intermediate (160–800 m) and shallow (above 160 m) layers, drawing in cold water from the Southern Ocean, which warms during its passage through the tropics and carries heat away at 30°N. In the Pacific and Indian Oceans, the overturning circulation is much weaker, so there is little net volume exchange with higher latitudes at any depth. But in all basins, there is a wind-driven subtropical gyre circulation, in which warm tropical water moves polewards in the boundary currents and cooler water is driven equatorwards across most of the basin. Overall, the Atlantic meridional flow produces a heat divergence of $0.57\,W\,m^{-2}$ above 160 m and 0.36 between 160 m and 800 m; for the Pacific and Indian Oceans together the figures are 1.00 and 1.04.

In addition to the effect of meridional divergence, the low-latitude oceans are also influenced by the influx of deep water from higher latitudes, which enters the deep layers and upwells into intermediate layers, cooling both

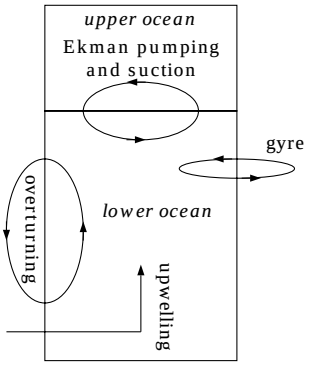

Fig. 15 Schematic showing circulations relevant to advective heat transport at low latitudes. The separation of upwelling from meridional overturning is artificial, but convenient for discussion. In fact the circulation must be closed, although this is not shown

as a result. In the Atlantic, deep water cools the ocean below 800 m by $0.05\,W\,m^{-2}$, and the layers between 160 m and 800 m by $0.16\,W\,m^{-2}$. In the Pacific and Indian Oceans, the corresponding figures are 0.28 and 0.10. By comparison with the previous paragraph we see that although upwelling does contribute to the cooling of the lower ocean, it is considerably less important than meridional heat divergence. This is at variance with the idea of the upwelling–diffusion model, which of course has no meridional transport. That model, however, would probably be assumed to include areas poleward of our 30° limits, which we chose because they delimit distinct regimes (Fig. 9).

At low latitudes in all oceans there is also an important advective heat exchange across 160 m as a result of the shallow wind-driven vertical circulation, with Ekman suction near the Equator and Ekman pumping polewards of 15° (Fig. 12) caused by the trade winds. The temperature contrast between shallow waters in the upward and downward branches of this meridional overturning is fairly weak. The main reason for net downward heat transport is that the vertical recirculation exchanges warm surface water with subsurface water which is being cooled more strongly, as we have seen, by meridional heat divergence and cold upwelling. The resulting heat flux across 160 m is $0.34\,W\,m^{-2}$ in the Atlantic, compensating for about a half of the advective cooling, and $0.38\,W\,m^{-2}$ in the Pacific and Indian Oceans. Hence the lower ocean has an overall advective heat loss, which maintains the vertical temperature gradient, and the heat budget is closed by the downward vertical diffusive heat flux from the surface layers.

In the anomaly experiment, the ocean below 160 m at low latitudes warms up mainly because of a 40% reduction (on the global average) in net advective cooling. By altering $\mathbf{v}$ and T separately and recalculating the advective heat fluxes by the method of Appendix B, we can describe how the change comes about. We find that temperature changes have only minor effects on the advective heat fluxes below 160 m, while alterations to the velocity field also have relatively little effect on the meridional heat divergence. The major change to advective heating results from reduced production of North Atlantic Deep Water and Antarctic Bottom Water, so average upward velocities throughout the water column become less. This strengthens the net downward velocity at 160 m, increasing the heat flux by $0.18\,W\,m^{-2}$, and it reduces the cooling effect of deep water entering the lower ocean. Upwelling across 800 m in the Atlantic declines from 2.9 Sv to 0.8 and in the Pacific and Indian from 2.2 to 0.3; cooling of the ocean below 160 m is consequently reduced by $0.36\,W\,m^{-2}$ (0.19 in the Pacific and Indian, 0.17 in the Atlantic). Hence, weaker upwelling, in concert with a small increase in meridional heat divergence, explains the $0.50\,W\,m^{-2}$ diagnosed as the contribution of advective changes to low-latitude heat uptake (Table 1).

Warming of the ocean by diffusion is little changed in the anomaly experiment. The control has a vertical temperature gradient of about $0.03\,K\,m^{-1}$ at low latitudes and 160 m. Climate change causes only a small fractional increase in the gradient of on the order of $10^{-3}\,K\,m^{-1}$, so the downward diffusive heat flux rises by $0.1\,W\,m^{-2}$, a 7% change. The reduction in advective cooling is hence the dominant term in the net warming.

Reduced upwelling in the Atlantic is the result of the weakening of the thermohaline circulation. In Sect. 6, we noted that this change led to a reduction of $\sim 0.1\,W\,m^{-2}$ in heat uptake below 160 m in the north Atlantic. But here we have found that it causes a reduction of $\sim 0.2\,W\,m^{-2}$ in cooling by upwelling at lower latitudes, and hence an increase in heat storage. In HADCM2, therefore, the net effect of the slowing of the Atlantic thermohaline circulation is to *increase* the heat uptake. This is consistent with the conclusions of Murphy (1995).

8 Conclusions

The rate of change of climate is determined jointly by the climate sensitivity and the processes which remove heat from the upper ocean. Motivated by an analysis of the time-dependence of ocean temperatures, we examine the vertical heat fluxes at 160 m depth in order to identify the mechanisms of heat uptake by the lower ocean on time scales of decades. As the control climate is a steady state, it shows a balance of upward and downward heat fluxes; during climate change, an imbalance develops, because the different processes have disparate feedback strengths and characteristic time scales of adjustment. The imbalance has different causes at low and high latitudes.

The Southern Ocean dominates both the vertical heat exchange in the control climate and the heat uptake during climate change. In HADCM2, the Deacon cell, which is a wind-driven overturning circulation, pumps heat downwards, balanced by diffusion and by convection in the upper few hundred metres. The effect of salinity on density allows temperature gradients to develop on isopycnal surfaces, causing heat to diffuse upward from the deep ocean, even though this is against the local vertical temperature gradient. Downward advection and upward diffusion is the reverse of the balance in the widely used global average upwelling–diffusion ocean model, implying that it may be inappropriate to rely on that model for a physical explanation of heat uptake in climate change. Nonetheless, as shown by Kattenberg et al. (1996), Raper and Cubasch (1996) and Raper et al. (Submitted 2000), an upwelling–diffusion model can be successfully calibrated to reproduce AOGCM results for heat uptake and temperature change.

As the climate warms, convection weakens in the upper layers of the Southern Ocean. A subsurface warming develops, reducing the isopycnal temperature gradients and restricting the diffusive loss of heat, while

the overturning circulation continues to transport heat downwards. This leads to a net increase in heat storage. In the northern oceans, the reduction of convection is the dominant process leading to accumulation of heat in the deep ocean, and to a weakening of the north Atlantic thermohaline circulation.

Deep water is formed at high latitudes but upwells in low latitudes, where its cooling effect is balanced in the control climate by downward diapycnal diffusion of heat. In both hemispheres, deep water formation is less in the anomaly climate. The consequent reduction of upwelling leads to a net uptake of heat in low latitudes as well, and is a more important effect than local heat uptake by diffusion. The increased heat storage in low latitudes is thus a result of changes at high latitudes. Through this indirect influence and through the direct transfer of heat by convection and diffusion between the upper and lower layers, the high-latitude regions play the principal role in determining the rate of uptake of heat by the global ocean, and hence in regulating the rate of climate change.

The correct representation of sub-grid-scale transports, parametrised by diffusion in HADCM2, is a topic of current interest in the development of climate models. The dependence of our results on diffusion is evidence that this emphasis is fully justified. Our newly developed HADCM3 model incorporates the scheme of Gent and McWilliams (1990) which we may expect will have a substantial role to play in its heat transports. Several authors (England 1995; Robitaille and Weaver 1995; Hirst et al. 1996a; Power and Hirst 1997; Wiebe and Weaver 1999) have shown that inclusion of this scheme can make large differences to uptake of passive tracers and heat. On a related point, Wiebe and Weaver (1999) found that the eddy velocities produced by the scheme of Gent and McWilliams (1990) cancelled out the large-scale velocities of the Deacon cell, which are of great importance to advective heat transport in HADCM2. We will therefore analyse climate change in HADCM3 following similar methods to those used in this work to establish how the conclusions are affected.

Acknowledgements I am most grateful to James Murphy, John Mitchell, Helene Banks, Richard Wood, Eric Guilyardi, Jason Lowe, Sarah Raper, David Marshall, Trevor McDougall and John Church for useful discussion and comments, and also to the two referees for their reviews. This work was supported by the UK Department of the Environment, Transport and the Regions under contract PECD 7/12/37 and by the Public Meteorological Service Research and Development Programme.

Appendix A: Two-layer ocean model

In this Appendix, we discuss a two-layer model of the ocean with a choice of parameters appropriate to the HADCM2 experiments, in order to demonstrate why it is reasonable to expect heating rates in the upper ocean to correlate with fluctuations in the surface net heat flux, while the lower ocean follows the linear surface trend.

Suppose the surface flux H (per unit area) is absorbed within an upper layer of thickness d_u, overlying a lower layer of thickness d_l. Temperatures are not necessarily uniform within the layers, but temperature variations are coherent and represented by $T_\mathrm{u}(t), T_\mathrm{l}(t)$, where t is time. The upper layer loses heat to the lower layer at a rate $k(T_\mathrm{u} - T_\mathrm{l})$, k being a constant. This term is a linear representation of heat transport by all processes, which we will take as a reasonable approximation for small perturbations from the steady state. The system is

$$\begin{aligned} c d_\mathrm{u} \frac{\mathrm{d}T_\mathrm{u}}{\mathrm{d}t} &= H - k(T_\mathrm{u} - T_\mathrm{l}) \\ c d_\mathrm{l} \frac{\mathrm{d}T_\mathrm{l}}{\mathrm{d}t} &= k(T_\mathrm{u} - T_\mathrm{l}) \end{aligned} \tag{5}$$

where c is the volumetric heat capacity. When this system is forced with a sinusoidally varying heat flux with angular frequency ω and amplitude $|H|$, the temperatures oscillate with amplitudes

$$\begin{aligned} |T_\mathrm{u}| &= \frac{|H|}{c\omega} \left(\frac{(c\omega d_\mathrm{l})^2 + k^2}{(c\omega d_\mathrm{u} d_\mathrm{l})^2 + k^2 (d_\mathrm{u} + d_\mathrm{l})^2} \right)^{\frac{1}{2}} \\ |T_\mathrm{l}| &= \frac{k|H|}{c\omega} \left((c\omega d_\mathrm{u} d_\mathrm{l})^2 + k^2 (d_\mathrm{u} + d_\mathrm{l})^2 \right)^{-\frac{1}{2}} . \end{aligned} \tag{6}$$

On the basis of the correlations discussed in Sect. 2 (Fig. 3), we take the upper layer as having a depth $d_\mathrm{u} \simeq 150$ m, and we will regard the layers beneath, down to the base of layer 15, as the lower ocean, giving $d_\mathrm{l} \simeq 2400$ m. Below this depth, the ocean is increasingly restricted to isolated basins. To estimate k, we use decadal means from the anomaly experiment to regress the rate of change of heat content of the lower ocean (layers 9 to 15 inclusive) against the change in the temperature difference between upper and lower ocean. This is a good straight line, passing close to the origin, with a correlation coefficient of 0.98, confirming that $k(T_\mathrm{u} - T_\mathrm{l})$ is an adequate parametrisation. The slope is $k = 1.6\,\mathrm{W\,m^{-2}\,K^{-1}}$. With $c = 4 \times 10^6\,\mathrm{J\,m^{-3}\,K^{-1}}$ and $\omega = 2 \times 10^{-8}\,\mathrm{s^{-1}}$, appropriate to periods of a decade, $(c\omega d_\mathrm{l})^2 \gg k^2$, so

$$|T_\mathrm{u}| = \frac{|H|}{c\omega d_\mathrm{u}} \quad |T_\mathrm{l}| = \frac{k|H|}{c\omega} \frac{1}{c\omega d_\mathrm{u} d_\mathrm{l}} = \frac{k}{c\omega d_\mathrm{l}} |T_\mathrm{u}| \ll |T_\mathrm{u}| \ , \tag{7}$$

which means that the upper ocean exhibits temperature fluctuations of the size expected for its heat capacity $c d_\mathrm{u}$, while the lower ocean's temperature fluctuates very little. For oscillations of this frequency, the two are almost disconnected. The phase of the upper-ocean temperature oscillation, with respect to that of the heat flux, is

$$\begin{aligned} \arg T_\mathrm{u} &= \tan^{-1} - \frac{(c\omega d_\mathrm{l})^2 d_\mathrm{u} + k^2 (d_\mathrm{u} + d_\mathrm{l})}{k c \omega d_\mathrm{l}^2} \\ &\simeq \tan^{-1} - \frac{c\omega d_\mathrm{u}}{k} \ . \end{aligned} \tag{8}$$

Since $c\omega d_\mathrm{u}$ is an order of magnitude larger than k, T_u is almost 90° behind H, so the heating rate $\mathrm{d}T_\mathrm{u}/\mathrm{d}t$ is in phase with the heat flux H.

Let us split up the time-dependence of the decadal average surface heat flux into a function which increases linearly with time, obtained from a least-squares fit, and the deviations from this function. The deviations are substantial compared with the average heating rate of the upper ocean. On account of this the time-dependence of the upper ocean heating rate is dominated by the fluctuations. Since the upper ocean responds on the decadal time scale, heating rates in layers 1–7 are in phase and correlate fairly strongly with the deviations in surface heat flux (Fig. 3). The fluctuations are smoothed out by the buffering effect of the upper ocean, so the lower ocean does not correlate with the deviations.

Turning to the long-term behaviour, we consider forcing the system of Eq. 5 with a heat flux $H(t) = Rt$ that increases linearly with time, R constant. The solution with $T_\mathrm{u}(0) = T_\mathrm{l}(0) = 0$ is

$$T_u = \frac{R}{2c(d_u+d_l)}t^2 + \frac{Rd_l^2}{k(d_u+d_l)^2}t - \frac{Rcd_ud_l^3}{k^2(d_u+d_l)^3} \times \left(1-\exp\left(-\frac{k}{c}\frac{d_u+d_l}{d_ud_l}t\right)\right)$$
$$T_l = \frac{R}{2c(d_u+d_l)}t^2 - \frac{Rd_ud_l}{k(d_u+d_l)^2}t + \frac{Rcd_u^2d_l^2}{k^2(d_u+d_l)^3} \times \left(1-\exp\left(-\frac{k}{c}\frac{d_u+d_l}{d_ud_l}t\right)\right) \quad (9)$$

For $d_l \gg d_u$, these approximate to

$$T_u = \frac{R}{2cd_l}t^2 + \frac{R}{k}t - \frac{Rcd_u}{k^2}\left(1-\exp\left(-\frac{kt}{cd_u}\right)\right)$$
$$T_l = \frac{R}{2cd_l}t^2 - \frac{Rd_u}{kd_l}t + \frac{Rcd_u^2}{k^2d_l}\left(1-\exp\left(-\frac{kt}{cd_u}\right)\right) \quad (10)$$

giving heating rates

$$\frac{dT_u}{dt} = \frac{R}{cd_l}t + \frac{R}{k}\left(1-\exp\left(-\frac{kt}{cd_u}\right)\right)$$
$$\frac{dT_l}{dt} = \frac{R}{cd_l}t - \frac{Rd_u}{kd_l}\left(1+\exp\left(-\frac{kt}{cd_u}\right)\right) \quad . \quad (11)$$

The time constant in the exponential is 12 a, so this term becomes unimportant after a couple of decades, leaving

$$\frac{dT_u}{dt} = \frac{R}{cd_l}t + \frac{R}{k} \quad \frac{dT_l}{dt} = \frac{R}{cd_l}t - \frac{Rd_u}{kd_l} \quad (12)$$

The straight-line fit to the time-development of the surface net heat flux in the anomaly experiment (Fig. 4) gives $R \sim 7\times 10^{-10}\,\mathrm{W\,m^{-2}\,s^{-1}}$. With the other the constants as above, the coefficient of t in the linear terms of Eq. 12 is about $7\times10^{-5}\,\mathrm{Ka^{-2}}$.

The constant in the upper-ocean heating rate is $0.014\,\mathrm{Ka^{-1}}$, which is twice as large as the linear term even after 80 years. Hence the upper-ocean heating rate fluctuates about a roughly constant value and does not correlate (layers 1–8) with the linearly increasing fit to the heat flux (Fig. 3). A constant heating rate means the upper-ocean temperature rises linearly with t (Fig. 6).

In the lower-ocean heating rate, the constant term has an additional factor d_u/d_l, making it more than an order of magnitude smaller. Hence the linear term dominates after the first decade or two. The lower-ocean heating rate therefore increases linearly with time and correlates well (below layer 8) with the trend of the surface heat flux (Fig. 3). Below layer 15, which we took as the base of the lower ocean, the heating rate is again less strongly correlated with the surface heat flux.

Appendix B: Interpretation of the advective heat flux

A 3D grid-point model such as HADCM2 naturally leads to an Eulerian view of advective heating: the average temperature of the water in a three-dimensional grid-box of the model is changed by advection if the water entering the box has a different temperature from the water leaving it. To answer the question of where the heat is coming from, we need an interpretation of the advective heat flux $\mathbf{v}T$ ($\mathbf{v}$ velocity, T temperature). This is problematic because of the continuity condition $\nabla\cdot\mathbf{v}=0$, which is a consequence of incompressibility.

Consider any enclosed volume within the ocean. If there is a flow into this volume anywhere across its surface, there will be an advective heat flux into the volume. But, by continuity, there must be a balancing flow out of the volume somewhere else on the surface, and this will necessarily have an associated heat flux as well. This is different from diffusion, since the presence of a diffusive heat flux somewhere across the surface does not imply anything at all about the existence of other diffusive heat fluxes elsewhere. For diffusion, portions of the surface can be considered independently, but the effect of advection can only be assessed by considering the inflow and outflow together, since the inward heat flux may be offset by the outward heat flux. If the flow is U ($\mathrm{m^3\,s^{-1}}$), the average inflow temperature T_i and the average outflow temperature T_o, the heat convergence due to the flow is $cU(T_i-T_o)$ (in units of power). It is not useful to consider the fluxes cUT_i and cUT_o separately, as we can see by supposing that $T_i=T_o$. As U varies, the inward heat flux can assume a range of values, but that does not mean that the volume is being heated more or less by advection, since no heat is deposited in any case. It is also obvious that cUT must be physically meaningless, because it is affected by the arbitrary choice of the zero of temperature. The main argument, however, results from continuity, and applies equally to any other tracer, such as salinity. The salt flux ρUS ($\mathrm{kg\,s^{-1}}$) is meaningful, but irrelevant, since changes of salinity are brought about, again, only by the difference between inflow and outflow.

The inflow and outflow through the surface are not generally in the same direction. Hence, one cannot evaluate heat convergence in x, y or z separately. We can illustrate this by considering the volume below a certain depth and north of a certain latitude extending right across an ocean basin which is closed at the north. Suppose there is sinking into the volume over its longitude–latitude face, balanced by a flow southward out of its latitude–depth face (the other faces are all closed off). If the inflow and outflow are at different average temperatures, there is a convergence of heat in the volume, but obviously we cannot say that this is due to either vertical or meridional flow separately. It is an effect of both together. Yet we have an intuition that there should be some sense in which we can identify the direction the heat is coming from. The idea behind this is that the heat budget of a given volume will respond in different ways to alterations to the velocity and temperature over its various surfaces. For instance, if there is an inflow of warm water through some portion of the surface, we expect that increasing the flow or raising its temperature will heat the water inside.

We can make our calculation of the heat fluxes match this intuition by using the volume average temperature T_{av} as a reference. For instance, considering a cuboidal volume with faces parallel to the coordinate axes, we can say that the heat flux across a longitude–depth face is $c\oint v(T_y-T_{av})\mathrm{d}x\,\mathrm{d}z$. If $T_y > T_{av}$, this is a flow of "warm" water (as regards this box), which would be heating it by flowing into the south face (for $v>0$), or cooling it by flowing out of the north face. Changing v or T_y will alter its effect in the way we expect. Of course, this flow must be balanced elsewhere to preserve continuity. Suppose a warm inflow at the south is balanced by an outflow at the top of the box at the average temperature. Then the heat flux through the top face $c\oint w(T_z-T_{av})\mathrm{d}x\,\mathrm{d}y=0$. This accords with our intuition: if we increase the throughflow, the box heats up because of increased input at the southern face, and not because of the consequent increase in upwelling through the top.

The heat fluxes seem to make sense individually, but this is only within the context of a particular state. In this case, T_{av} will slowly rise because of the increased heat convergence, presuming that it was in a steady state initially with advective convergence balanced by, for instance, diffusive heat loss. If the heat losses do not change, we might eventually reach a state in which the average temperature is that of the southern inflow $T_y=T_{av}$, and $T_z<T_{av}$ for the outflow. The heat convergence is unchanged, but now it appears that the heating is caused by the removal of cold water through the top face, with the southern face having no heat input. This shows that reference to T_{av} is useful in helping to understand the effect of perturbations in $\mathbf{v}$ and T on the heat budget of individual boxes, but the decomposition into components is still arbitrary.

Moreover, since boxes have different T_{av}, a flux from one box to an adjacent box does not have equal and opposite effects on the two boxes. If the box to the south in the example above has a higher average temperature ($>T_y$), the northward flow out of the box is heating it up, by removing cooler water. This same flow is also heating the box to the north, by adding warmer water. The decomposition will only help us, therefore, with understanding the temperature in an individual box, and not its relation to its neighbours.

The vertical, meridional or zonal advective heat flux separately is only well defined if there is zero velocity through all surfaces except one. Thus, if we have an enclosed basin, we know that all flow passing through a vertical plane from top to bottom along a line of latitude is meridional, so the heat flux across it must be meridional, and is well defined because we know that all flow which goes through the surface must come back through it. But we have no information about the variation with depth or longitude of the heat flux. This variation is undefined, because the heat flux is, as before, not a property separately of the inflow or the outflow (which occur at different depth and longitude), but of the connection between them. Similarly, we can evaluate the vertical heat flux for the basin at any depth (or for the whole world, which is completely enclosed), but there is no information about its geographical distribution.

References

Boer GJ, Flato G, Ramsden D (2000) A transient climate change simulation with greenhouse gases and aerosol forcing: projected climate for the 21st century. Clim Dyn In press

Bretherton FP, Bryan K, Woods JD (1990) Time-dependent greenhouse-gas-induced climate change. In: Houghton JT, Jenkins GJ, Ephraums JJ (eds) Climate change: the IPCC scientific assessment. Cambridge University Press, Cambridge, UK, pp 173–193

Bryan K (1996) The steric component of sea level rise associated with enhanced greenhouse warming: a model study. Clim Dyn 12: 545–555

Bryden HL (1993) Ocean heat transport across 24N latitude. In: McBean GA, Hantel M (eds) Interactions between global climate subsystems: the legacy of Hann, vol. 75 of Geophysical Monographs, pp 65–75

Colman RA, Power SB, McAvaney BJ, Dahni RR (1995) A non-flux-corrected transient CO_2 experiment using the BMRC coupled atmosphere/ocean GCM. Geophys Res Lett 22: 3047–3050

Cox MD (1984) A primitive equation, three dimensional model of the ocean. Ocean Group Technical Report 1, GFDL Princeton, USA

Cubasch U, Hasselmann K, Höck H, Maier-Reimer E, Mikolajewicz U, Santer BD, Sausen R (1992) Time-dependent greenhouse warming computations with a coupled ocean-atmosphere model. Clim Dyn 8: 55–69

Döös K, Webb DJ (1994) The Deacon cell and the other meridional cells of the Southern Ocean. J Phys Oceanogr 24: 429–442

England MH (1995) Using chlorofluorocarbons to assess ocean climate models. Geophys Res Lett 22: 3051–3054

Fanning AF, Weaver AJ (1997) A horizontal resolution and parameter sensitivity study of heat transport in an idealized coupled climate model. J Clim 10: 2469–2478

Gates WL, Mitchell JFB, Boer GJ, Cubasch U, Meleshko VP (1992) Climate modelling, climate prediction and model validation. In: Houghton JT, Callander BA, Varney SK (eds) Climate change 1992: the supplementary report to the IPCC scientific assessment. Cambridge University Press, Cambridge, pp 97–134

Gent PR, McWilliams JC (1990) Isopycnal mixing in ocean circulation models. J Phys Oceanogr 20: 150–155

Gill AE (1982) Atmosphere–ocean dynamics. Academic Press, New York, pp 662

Gordon HB, O'Farrell SP (1997) Transient climate change in the CSIRO coupled model with dynamic sea ice. Mon Weather Rev 125: 875–907

Gregory JM, Mitchell JFB (1997) The climate response to CO_2 of the Hadley Centre coupled AOGCM with and without flux adjustment. Geophys Res Lett 24: 1943–1946

Guilyardi E, Madec G, Terray L (1999) The role of lateral ocean physics in the upper ocean thermal balance of a coupled ocean-atmosphere GCM. J Phys Oceanogr (in press)

Hall MM, Bryden HL (1982) Direct estimates and mechanisms of ocean heat transport. Deep-Sea Res 29: 339–359

Haywood JM, Stouffer RJ, Wetherald RT, Manabe S, Ramaswamy V (1997) Transient response of a coupled model to estimated changes in greenhouse gas and sulfate concentrations. Geophys Res Lett 24: 1335–1338

Hirst AC, Gordon HB, O'Farrell SP (1996a) Global warming in a coupled climate model including oceanic eddy-induced advection. Geophys Res Lett 23: 3361–3364

Hirst AC, Jackett DJ, McDougall TJ (1996b) The meridional overturning cells of a world ocean model in neutral density coordinates. J Phys Oceanogr 26: 775–791

Hoffert MI, Callegari AJ, Hsieh CT (1980) The role of deep sea heat storage in the secular response to climate forcing. J Geophys Res 85: 6667–6679

Johns TC, Carnell RE, Crossley JF, Gregory JM, Mitchell JFB, Senior CA, Tett SFB, Wood RA (1997) The second Hadley Centre coupled ocean-atmosphere GCM: model description, spinup and validation. Clim Dyn 13: 103–134

Karoly DJ, McIntosh PC, Berrisford P, McDougall TJ, Hirst AC (1997) Similarities of the Deacon cell in the Southern Ocean and Ferrel cells in the atmosphere. Q J R Meteorol Soc 123: 519–526

Kattenberg A, Giorgi F, Grassl H, Meehl GA, Mitchell JFB, Stouffer RJ, Tokioka T, Weaver AJ, Wigley TML (1996) Climate models—projections of future climate. In: Houghton JT, Meira Filho LG, Callander BA, Harris N, Kattenberg A, Maskell K (eds) Climate change 1995. The science of climate change. Cambridge University Press, Cambridge, UK, pp 285–358

Keen AB, Murphy JM (1997) Influence of natural variability and the cold start problem on the simulated transient response to increasing CO_2. Clim Dyn 13: 847–864

Kraus EB, Turner JS (1967) A one dimensional model of the seasonal thermocline. Part II. Tellus 19: 98–105

Manabe S, Stouffer RJ (1994) Multiple century response of a coupled ocean-atmosphere model to an increase of atmospheric carbon dioxide. J Clim 7: 5–23

Manabe S, Stouffer RJ, Spelman MJ, Bryan K (1991) Transient responses of a coupled ocean-atmosphere model to gradual changes of atmospheric CO_2. Part I: annual mean response. J Clim 4(8): 785–818

McDougall TJ (1987) Neutral surfaces. J Phys Oceanogr 17: 1950–1964

Meehl GA, Washington WM (1996) El Niño-like climate change in a model with increased atmospheric CO_2 concentrations. Nature 382: 56–60

Mikolajewicz U, Voss R (1998) The role of the individual air-sea flux components in CO_2-induced changes of the ocean's circulation and climate. Report 263, Max-Planck-Institut für Meteorologie, Hamburg, Germany

Mitchell JFB, Manabe S, Meleshko V, Tokioka T (1990) Equilibrium climate change—and its implications for the future. In: Houghton JT, Jenkins GJ, Ephraums JJ (eds) Climate change: the IPCC scientific assessment. Cambridge University Press, Cambridge, UK, pp 131–172

Mitchell JFB, Johns TC, Gregory JM, Tett SFB (1995) Climate response to increasing levels of greenhouse gases and sulphate aerosols. Nature 376: 501–504

Murphy JM, Mitchell JFB (1995) Transient response of the Hadley Centre coupled ocean-atmosphere model to increasing carbon dioxide. Part II: spatial and temporal structure of response. J Clim 8: 57–80

Murphy JM (1995) Transient response of the Hadley Centre coupled ocean-atmosphere model to increasing carbon dioxide: Part III. Analysis of global-mean response using simple models. J Clim 8: 496–514

Osborn TJ (1998) The vertical component of epineutral diffusion and the dianeutral component of horizontal diffusion. J Phys Oceanogr 28: 485–494

Power SB, Hirst A (1997) Eddy parametrization and the oceanic response to idealized global warming. Clim Dyn 13: 417–428

Rahmstorf S (1996) On the freshwater forcing and transport of the atlantic thermohaline circulation. Clim Dyn 12: 799–811

Raper SCB, Cubasch U (1996) Emulation of the results from a coupled general circulation model using a simple climate model. Geophys Res Lett 23: 1107–1110

Raper SCB, Gregory JM, Osborn TJ (2000) Use of an upwelling-diffusion energy balance climate model to simulate and diagnose A/OGCM results. Clim Dyn Submitted

Robitaille DY, Weaver AJ (1995) Validation of sub-grid-scale mixing schemes using CFCs in a global ocean model. Geophys Res Lett 22: 2917–2920

Russell GL, Miller JR, Rind D (1995) A coupled atmosphere-ocean model for transient climate change studies. Atmos Ocean 33: 683–730

Schlesinger ME, Jiang X (1990) Simple model representation of atmosphere-ocean gcms and estimation of the timescale of CO_2-induced climate change. J Clim 3: 1297–1315

Senior CA, Mitchell JFB (2000) The time dependence of climate sensitivity. Geophys Res Lett Submitted

Weaver AJ, Bitz CM, Fanning AF, Holland MM (1999) Thermohaline circulation: high-latitude phenomena and the difference between the Pacific and Atlantic. Annu Rev Earth Planet Sci 27: 231–285

Wiebe EC, Weaver AJ (1999) On the sensitivity of global warming experiments to the parametrisation of sub-grid scale ocean mixing. Clim Dyn 15: 875–893

Wigley TML, Raper SCB (1992) Implications for climate and sea level of revised IPCC emissions scenarios. Nature 357: 293–300

Wood RA, Keen AB, Mitchell JFB, Gregory JM (1999) Changing spatial structure of the thermohaline circulation in response to atmospheric CO_2 forcing in a climate model. Nature 399: 572–575